

## Small Molecule Solution-Processed Bulk Heterojunction Solar Cells<sup>†</sup>

Bright Walker, Chunki Kim, and Thuc-Quyen Nguyen\*

*Departments of Chemistry and Biochemistry, Institute for Polymers and Organic Solids,  
University of California, Santa Barbara, California 93106, United States*

*Received August 2, 2010. Revised Manuscript Received October 4, 2010*

Although most research in the field of organic bulk heterojunction solar cells has focused on combinations of a p-type conducting polymer as a donor and a fullerene-based acceptor, recent work has demonstrated the viability of solution-processed heterojunctions composed entirely of molecular solids. Molecular solids offer potential advantages over conjugated polymer systems in terms of easier purification, amenability to mass-scale production and better batch-to-batch reproducibility. This article reviews the major classes of molecular donors that have been reported in the literature in the past several years and highlights some of key considerations in molecular heterojunction design compared to polymer-based bulk heterojunctions.

### Introduction

There is a general preconception in the field of organic photovoltaic (OPV) research that organic bulk heterojunction (BHJ) solar cells consist of a phase-separated mixture of a p-type conjugated polymer as a donor and the fullerene derivative phenyl-C<sub>61</sub>-butyric acid methyl ester (PCBM) as an acceptor. This preconception is supported by the vast majority of OPV literature which has focused on this type of system.<sup>1</sup> Although this has so far been the most successful type of BHJ, with demonstrated power conversion efficiencies (PCEs) in excess of 7%,<sup>2</sup> there is no reason that the donor must be a polymer or that the acceptor must be a fullerene.

Frequently referred to as “polymer” solar cells, it seems that one often overlooked aspect of BHJ research is that the small molecule originally synthesized by Hummelen et al.<sup>3</sup> has largely filled the need for an n-type component in BHJs. Considering the wide range of donor materials that can be used with PCBM to successfully fabricate BHJ solar cells, it seems that PCBM could be considered the essential material which enables efficient power conversion in polymer solar cells more than any conjugated polymer. Considering the effectiveness of the PCBM molecule, and that polymers are generally more difficult to synthesize and purify than small molecules, one might wonder why until recently, there has not been more effort to discover a p-type (donor) analogue of PCBM, or more reports of BHJs comprising molecular donor materials.

One of the most appealing aspects of BHJ solar cells is that they can be deposited from solution like inks, enabling large-scale production by techniques like printing or roll-to-roll coating. Conjugated polymers lend themselves to solution processing due to their desirable film-forming properties, however, molecular solids can also be

processed in the same way. The term BHJ is often used to refer to a bicontinuous, interpenetrating network of donor and acceptor phases; however, when two low-molecular-weight solids are deposited from solution in a manner similar to polymer BHJs, the two materials may not form bicontinuously or interpenetrating as observed in polymer counterparts. Nonetheless, they may still produce a photovoltaic effect and we will refer to this type of system as a solution-processed molecular bulk heterojunction (SMBHJ<sup>4</sup>). This class of solar cell received relatively little attention prior to 2006, but has seen a growing body of research in recent years. Recent work has demonstrated that it is possible to solution-process BHJs comprising nonpolymeric donor and acceptor phases that are able to achieve PCEs comparable to some of the best known polymer systems,<sup>5</sup> such as poly 3-hexylthiophene (P3HT).<sup>6,7</sup> This review will briefly outline the development of SMBHJs and focus on some of the more recent successes in the field, highlighting outstanding results from representative classes of materials including oligothiophenes, acenes, diketopyrrolopyrroles and push–pull type oligomers, as well as a few other dye-based materials (see representative structures in Figure 1). For more information on the topic, the reader is encouraged to read existing SMBHJ reviews such as those written by Lloyd<sup>8</sup> and Roncali.<sup>9</sup>

### Original Work and Brief History of SMBHJs

Some of the first SMBHJs were reported a few years after the polymer BHJ concept was first reported<sup>10,11</sup> at a time when general interest in BHJ solar cells was beginning to accelerate. These included reports of solution processed phthalocyanine/perylene blends<sup>12</sup> and hexabenzocoronene (HBC)/perylene blends.<sup>13,14</sup> The reported phthalocyanine/perylene devices were prepared by spin-casting a mixed solution of compounds **1** and **2** in chloroform onto a transparent, conducting substrate, followed by evaporation of a metal cathode. These devices exhibited

<sup>†</sup> Accepted as part of the “Special Issue on  $\pi$ -Functional Materials”.

\*Corresponding author. E-mail: quyen@chem.ucsb.edu.

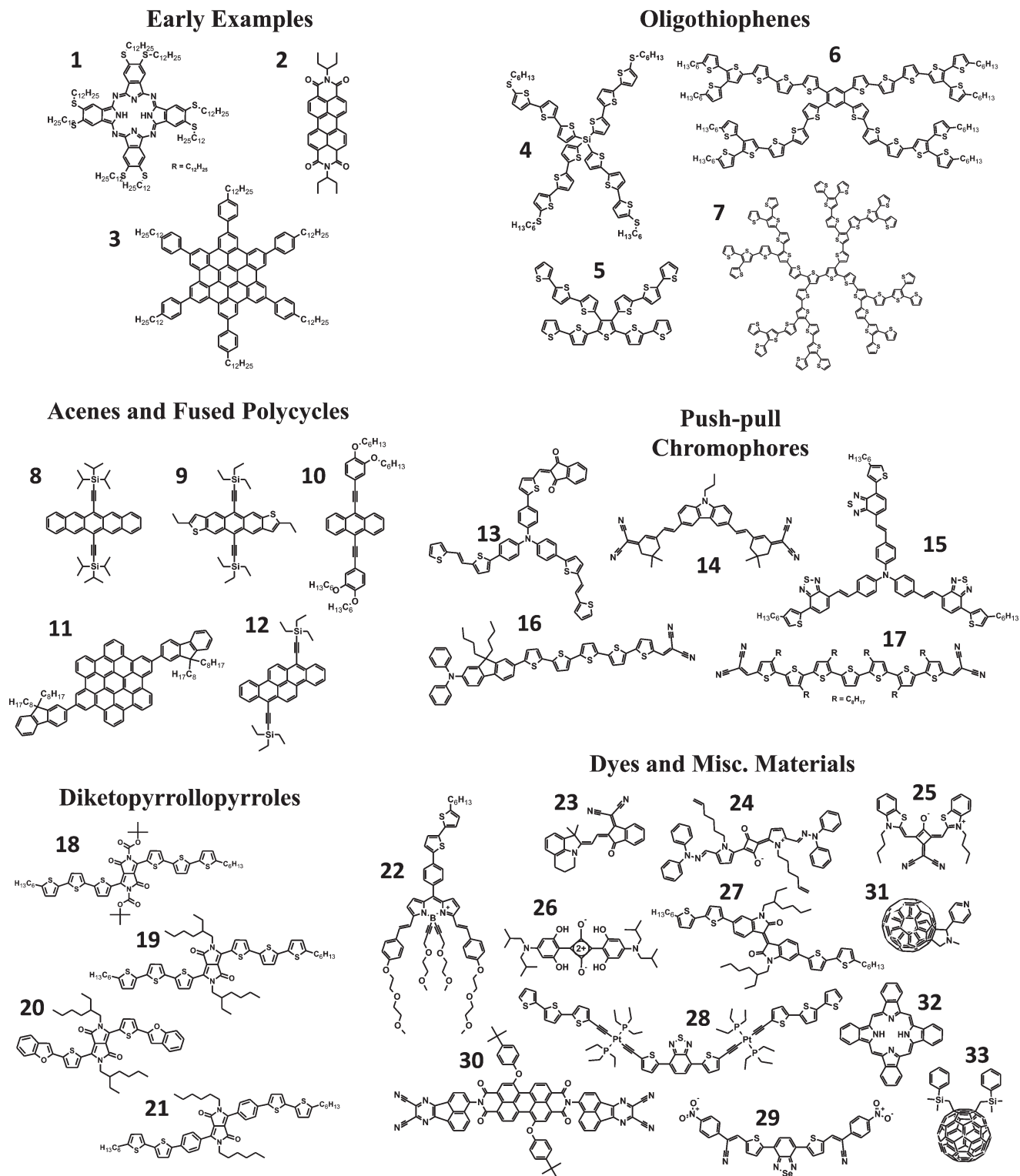


**Figure 1.** Examples of some most successful chemical structures reported in solution-processed organic solar cells using small molecules as donors reported in the literature.

poor device characteristics compared to known polymer systems at the time (Figure 2).

The HBC material **3** showed a promising ability to stack into ordered domains, with some tendency to form columns oriented perpendicular to the substrate surface.<sup>15</sup> This type of vertical phase separation is different from the phase separation apparent in polymer BHJs. In fact, this system may fall outside of the realm of structures normally encompassed by

the term “bulk” heterojunction. The unusual vertical ordering in this system presents an appealing prospect for efficient carrier transport. However, devices based on the donor **3** and perylene acceptor **2** did not demonstrate very impressive performance (short-circuit current density ( $J_{SC}$ ) = 33.5  $\mu\text{A}/\text{cm}^2$  and an open-circuit voltage ( $V_{OC}$ ) = 0.69 V).

The original SMBHJs did not show much promise as solar cell materials. Perhaps it was the rather disappointing

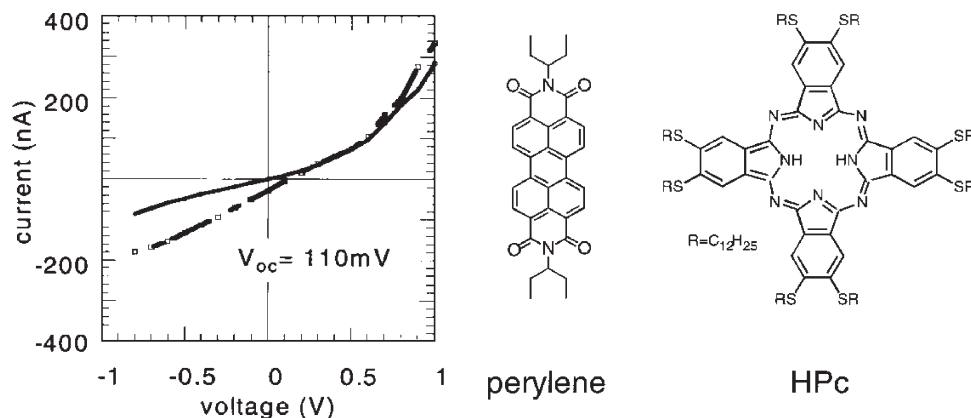


**Figure 2.** Current–voltage characteristics of the first reported SMBHJ device based on a phthalocyanine/perylene pair; this device produced a small photovoltaic effect. Reproduced with permission from ref 12. Copyright 2000 Elsevier.

**Table 1.** Summary of Results Obtained with Original SMBHJs

donor structure	acceptor	D:A ratio	donor MW (Da)	abs. onset (nm)	$J_{sc}$ (mA/cm <sup>2</sup> )	$V_{oc}$ (V)	FF (%)	PCE (%)	ref
1	2	1:1	2118	800 <sup>a</sup>	0.00075 <sup>b</sup>	0.11 <sup>b</sup>	25 <sup>b</sup>	$8.3 \times 10^{-3b}$	12
3	2	4:6	1989	620 <sup>a</sup>	0.0335 <sup>c</sup>	0.69 <sup>c</sup>	40 <sup>c</sup>	1.95 <sup>c</sup>	13

<sup>a</sup> Estimated from EQE. <sup>b</sup> Under monochromatic illumination at 650 nm and a power of 0.25 mW/cm<sup>2</sup>. <sup>c</sup> Under monochromatic illumination at 490 nm and a power of 0.47 mW/cm<sup>2</sup>.

performance reported in these initial works that discouraged research into SMBHJs for the next several years, as little new work with SMBHJs was reported again until early 2006 when papers by Roncali, Sun, Kopidakis and Lloyd marked a re-emergence of interest in the field.<sup>16–18</sup> Table 1 summarizes device results of some original SMBHJs.

### Oligothiophenes

Early in 2006, Roncali reported using branched oligothiophenes in solution processed BHJs with the intent of forming two- and three-dimensional conjugated networks of overlapping, star-shaped oligothiophenes.<sup>16,19,20</sup> The first SMBHJ reported by Roncali consisted of a silicon core with four terthiophene branches (structure 4) blended with PCBM and showed an absorption cutoff of 440 nm, corresponding to an optical band gap of about 2.8 eV. Although these devices did not perform as well as polymer BHJs at that time, they showed significant improvement over the few existing examples of SMBHJs with a  $J_{sc}$  of 1.15 mA/cm<sup>2</sup> and a PCE of 0.3% (under 80 mW/cm<sup>2</sup> illumination). Because this material is only able to absorb the violet and ultraviolet light fraction of the solar spectrum, large photocurrents are impossible; however, these initial results helped to establish the viability of SMBHJs.

Shortly after the first SMBHJ publication, Sun et al. reported the fabrication of SMBHJ solar cells using X-shaped oligothiophenes consisting of a tetrasubstituted thiophene core with oligothiophene branches of various lengths blended with PCBM.<sup>17</sup> In this work, the most promising material explored (structure 5) was the material with the longest oligothiophene chains. Atomic force microscopy (AFM) images of these compounds blended with PCBM showed that the material with the longest thiophene chains exhibited the smallest feature size (< 500 nm),

whereas UV–vis absorption spectra showed that it also had the lowest band gap with an absorption onset of 520 nm. Although the series resistance was not reported, the dark currents reveal larger currents at forward bias with increasing oligothiophene chain length, implying that longer chains result in lower series resistance. Devices prepared using a 45:55 mixture with PCBM showed a  $J_{sc}$  of 3.65 mA/cm<sup>2</sup>,  $V_{oc}$  of 0.85 V, fill factor (FF) of 26% and overall PCE of 0.8%.

The next SMBHJ was reported by Kopidakis et al. who published results using a series of X-shaped oligothiophenes with 1,3,5 or 1,2,4,5 substituted phenyl cores<sup>21</sup> using PCBM as an acceptor. Once again, the oligomers with highest molecular weight and longest oligothiophene chain length showed the best performance. The most promising material examined in this study (structure 6) consisted of a 1,2,4,5 substituted phenyl core with each arm consisting of six thiophene rings. Devices based on this material exhibited a  $J_{sc}$  of 3.35 mA/cm<sup>2</sup>,  $V_{oc}$  of 0.94 V, FF of 40% and overall PCE of 1.3%. The authors attributed the modest efficiency to poor phase separation.

Perhaps the most effective results with oligothiophenes were reported by Baurle and co-workers in 2008 using large, highly branched oligothiophene dendrimers blended with PCBM. The largest oligomers showed absorption cutoffs up to 600 nm. Optimized solar cells using structure 7 and PCBM produced a  $J_{sc}$  of 4.19 mA/cm<sup>2</sup>,  $V_{oc}$  of 0.97 V, FF of 42%, and PCE of 1.7%.<sup>22</sup> The molecular weights of the best performing dendrimers were between 3000–8000 Da; within the range of low-molecular-weight polymers.

In general, larger size and longer  $\pi$ -conjugation length in oligothiophenes seems to lead to better material properties and solar cell performance; the best results approach values that might be obtained using P3HT. Table 2 compares optoelectronic properties of each optimized system.

Table 2. Optoelectronic Properties of Optimized Oligothiophene Systems

donor structure	acceptor	D:A ratio	donor MW (Da)	thiophene conjugation <sup>a</sup>	abs. onset (nm)	$J_{sc}$ (mA/cm <sup>2</sup> )	$V_{oc}$ (V)	FF (%)	PCE (%)	ref
4	PC <sub>61</sub> BM	1:1.7	1354	3	440	1.41 <sup>b</sup>	0.85	24	0.3	16
5	PC <sub>61</sub> BM	1:1.2	905	5	520	3.65	0.85	26	0.8	17
6	PC <sub>61</sub> BM	1:4	2722	5	550	3.35	0.94	40	1.3	21
7	PC <sub>61</sub> BM	1:2	3451	12	600	4.19	0.97	42	1.7	22

<sup>a</sup> Number of thiophene units with sequential 2,5 connectivity. <sup>b</sup> Normalized to 100 mW/cm<sup>2</sup> illumination intensity.

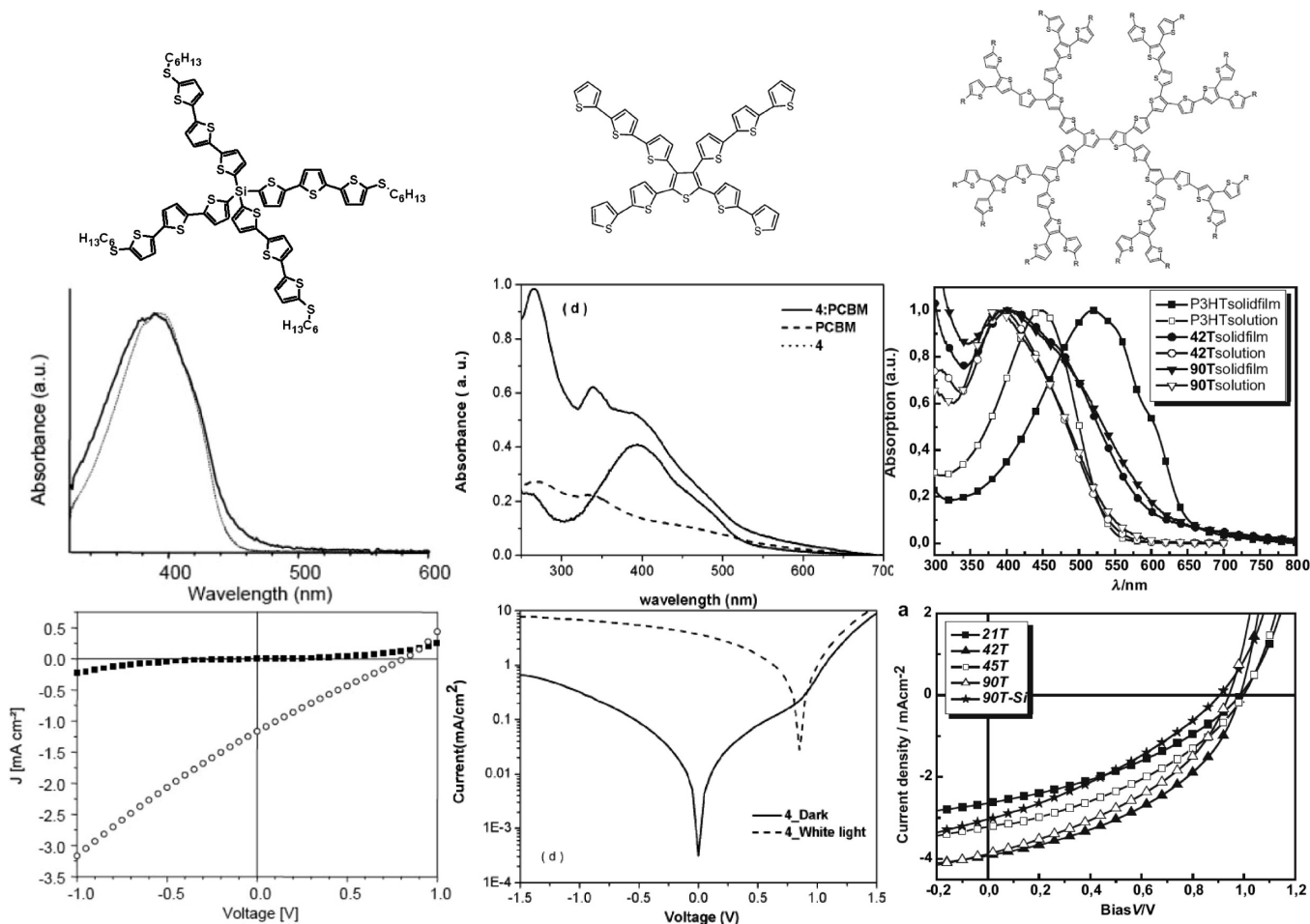


**Figure 3.** Comparison of oligothiophenes of various size and structure against their absorption spectra and current–voltage characteristics as SMBHJ devices with PCBM. As a general trend, oligothiophenes with longer  $\pi$ -conjugated chains linked in the 2,5 position tend to have lower band gaps and produce better devices. Reproduced with permission from ref 20, copyright 2006 Royal Society of Chemistry; ref 17, copyright 2006 American Chemical Society; and ref 22, copyright 2008 Wiley-VCH Verlag GmbH & Co. KGaA.

Figure 3 compares the structures, absorption spectra, and current–voltage characteristics of a few representative thiophene oligomers. It appears that the effective conjugation length and band gap are largely determined by the number of sequential thiophene rings linked in the 2,5 position, where the representative structures have 3, 5, and 12 thiophene units linked in this manner, resulting in absorption onsets of approximately 440 nm, 520 nm, and 600 nm, respectively and maximum reported PCEs of 0.3, 0.8, and 1.7%, respectively. These studies seem to indicate that it may not be possible to produce higher device efficiencies with linear, branched or star-shaped oligothiophenes than those obtained with P3HT.

### Soluble Acenes

Acenes and polycyclic arenes such as pentacene and rubrene are known to have properties that are very

attractive as donor materials in organic solar cells, including high charge carrier mobilities and broad absorption spectra.<sup>23–27</sup> This type of materials has been successfully used in thermally evaporated bilayer solar cells and has great potential for use in SMBHJs if the acenes are properly functionalized with solubilizing groups.

At about the same time that Roncali and co-workers were exploring 3D oligothiophenes, Malliaras and Anthony began work to develop solution processable p-type acenes. Their work led to the first publication of a solution processable pentacene derivative (structure 8) which was incorporated into modestly efficient bilayer devices with an evaporated C<sub>60</sub> layer in early 2006,<sup>18</sup> followed by SMBHJs using an anthradithiophene with triethylsilylethynyl appendages (structure 9) and PCBM.<sup>28</sup> The anthradithiophene



Table 3. Summary of Results with Fused Polycyclic Arene-Based SMBHJs

donor structure	acceptor	D:A ratio	donor MW (Da)	abs. onset (nm)	hole mobility ( $\text{cm}^2/(\text{V s})$ )	$J_{\text{sc}}$ ( $\text{mA}/\text{cm}^2$ )	$V_{\text{oc}}$ (V)	FF (%)	PCE (%)	ref
9	PC <sub>61</sub> BM	7:3	623	580	0.11 <sup>a</sup>	2.96	0.84	40	1.0	28
10	PC <sub>61</sub> BM	1:1.17	779	550	$4 \times 10^{-4b}$	3.34 <sup>c</sup>	0.762	44	1.12	33
10	PC <sub>61</sub> BM	2:1	779	550	$4 \times 10^{-4b}$	3.10	0.89	45	1.27	35
11	PC <sub>61</sub> BM	1:2	1300	470	$2.8 \times 10^{-4a}$	2.68	0.90	61	1.46	37
12	PC <sub>61</sub> BM	1:1	579	600		6.55	0.83	41	2.25	38

<sup>a</sup> Field effect mobility measured for blend film with PC<sub>61</sub>BM. <sup>b</sup> Field effect mobility measured for neat film. <sup>c</sup> Normalized to 100 mW/cm<sup>2</sup> illumination.

material shows an absorption cutoff of 575 nm in the solid state (with a HOMO of 5.15 eV and LUMO of 2.98 eV) and has an impressive hole mobility of up to 0.11  $\text{cm}^2/(\text{V s})$ .<sup>29</sup> The material forms fairly amorphous films with PCBM after spin-casting which do not generate large photocurrents, but can be induced to crystallize in “spherulite” type domains by exposure to solvent (toluene and chlorobenzene) vapor. After exposure to solvent vapor, the spherulite covered fraction of the film appears rough with submicrometer, needle-like crystals and shows a marked improvement in photocurrent generating capacity. The authors reported that the photocurrent generated by these devices was proportional to the area covered by spherulites; the best results were obtained with films having 82% spherulite coverage, which produced a  $J_{\text{SC}}$  of 2.96  $\text{mA}/\text{cm}^2$ ,  $V_{\text{OC}}$  of 0.84 V, FF of 0.4, and PCE of 1.0%.

Since the initial work with pentacene and anthradithiophene, pentacene derivatives have been extensively characterized including solid-state structures and relationships between crystal structure<sup>30</sup> and variations in molecular structure, such as solubilizing groups. The HOMO energy band has been modified with an increase the  $V_{\text{OC}}$ <sup>31</sup> by appending 1,3 dioxolane moieties to the pentacene structure. Additionally, n-type pentacene derivatives have been prepared for use as acceptors.<sup>32</sup>

Aside from the work done with pentacenes and anthradithiophenes, solar cells incorporating polycyclic arenes have been reported by other groups as well. For instance, SMBHJ devices incorporating an anthracene (structure 10) and PCBM were first reported by Valentini et al. in 2008 with a PCE of 1.1%.<sup>33</sup> In a subsequent report, the authors found that an acetylinic spacer yielded significantly better performance than an olefinic spacer in this type of system.<sup>34</sup> Recently, the authors reported on the investigation of a series of aryl acetylenes, similar to structure 10. In this study, field-effect transistors (FETs) were fabricated from each material to examine carrier transport. The materials exhibited field effect hole mobilities of up to 0.1  $\text{cm}^2/(\text{V s})$ , and the carrier mobilities were found to correlate well with photovoltaic performance. The most promising material was found to be the same material originally reported in 2008 (structure 10), which forms smooth films when spin-cast with PCBM and shows a tendency to form crystalline domains upon thermal annealing. Optimized devices produced a  $J_{\text{SC}}$  of 3.1  $\text{mA}/\text{cm}^2$ ,  $V_{\text{OC}}$  of 0.89 V, FF of 45%, and PCE of 1.27%.<sup>35</sup>

Although the first attempts to incorporate coronenes into SMBHJs in 2001 left some room for improvement, later work by Mullen and co-workers with the HBC system led to devices with peak external quantum efficiencies

(EQEs) of up to 29.5% in 2006,<sup>36</sup> and even more recently, work with a blend of fluorenyl substituted HBC (structure 11) and PCBM has been able to generate macroscopic  $J_{\text{SC}}$  and PCE of up to 2.68  $\text{mA}/\text{cm}^2$  and 1.46%, respectively.<sup>37</sup>

Perhaps the most successful results among fused aromatic polycycles were obtained by Winzenberg et al. in 2009<sup>38</sup> using a 1:1 mixture of an acetyl triethylsilyl substituted dibenzochrysene material (structure 12) and PCBM spin-casted from chloroform. The material exhibits a HOMO of 5.1 eV and a LUMO of 2.9 eV as determined from ultraviolet photoelectron spectroscopy (UPS) and UV-vis spectra. Spin-casted BHJ films are fairly smooth compared to other acenes, showing surface features larger than 1  $\mu\text{m}$  when chlorobenzene was used and smaller than 1  $\mu\text{m}$  when chloroform was used at high concentration and high spin speeds. It seems likely that the relatively small domain sizes achieved in this study provided a large interfacial area for carrier dissociation and contributed to a relatively large  $J_{\text{SC}}$  of 6.55  $\text{mA}/\text{cm}^2$  compared to other acenes. The optimized devices showed a  $V_{\text{OC}}$  of 0.83 V, FF of 0.41, and PCE of 2.3%.

From these studies of soluble acenes, it seems that this class of molecule has a strong tendency to crystallize into well-defined structures and transport carriers efficiently; however, domain sizes are too large with insufficient interfacial area to allow efficient exciton dissociation. Table 3 summarizes the results and Figure 4 compares the surface structure of three acenes used in SMBHJs. Although the size scales of each image are different, it can be seen that the surface features are largest in the anthradithiophene film and significantly smaller in the anthracene and dibenzochrysene films. The current densities in the latter two are much higher considering their absorption spectra.

### Push–Pull Chromophores

Although the term “push–pull chromophore” could be applied to many of the molecules described in this review (such as merocyanine dyes), we will limit discussion of this class of materials to structures containing an obvious push–pull structure including well-known electron donating moiety (such as triphenylamine or carbazole) and a well-known electron-withdrawing moiety (such as benzo-thiadiazole or dicyanovinylene) separated by a  $\pi$ -bridge (such as thienyl, vinyl, or phenyl moieties). This type of molecular architecture is very effective at producing low-band-gap materials where the HOMO and LUMO levels can be controlled and has become a common approach

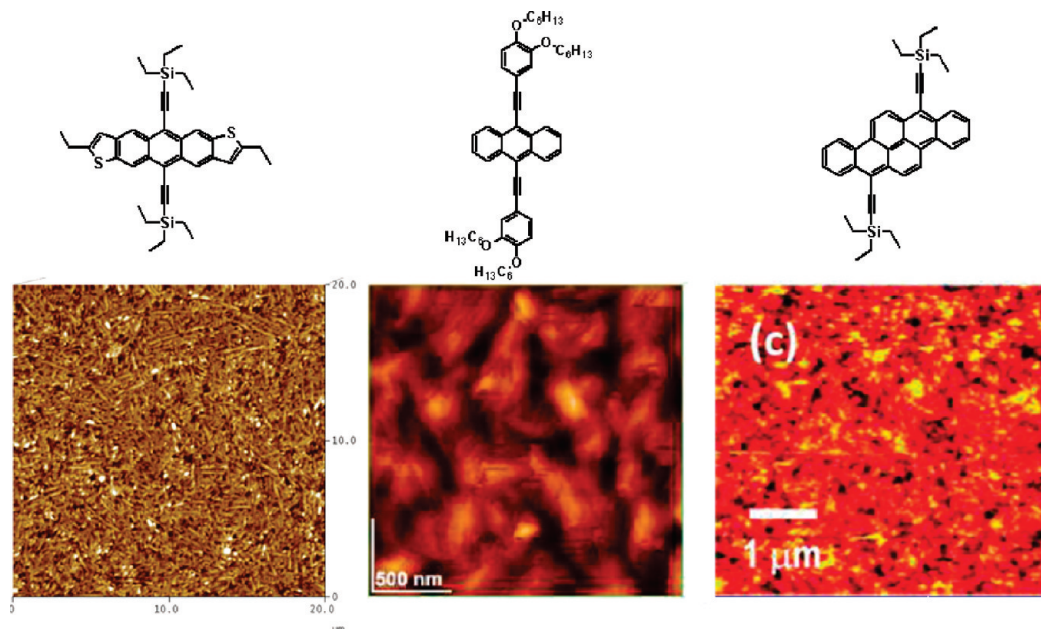


**Figure 4.** AFM images of acene SMBHJs based on structures **9**, **10**, and **12**. Antradiithiophene **9** shows the largest domain sizes and produces the lowest current densities based on its absorption spectrum. Reproduced with permission from ref 28, copyright 2007 American Chemical Society; ref 35, copyright 2010 American Chemical Society; and ref 38, copyright 2009 American Chemical Society.

for the design of materials with broad absorption for use in polymer solar cells.<sup>39–43</sup> It is also a very effective way to tailor molecular donors as evidenced by the numerous reports on this type of material published in the past 3 years.

The first SMBHJs incorporating push–pull molecules were reported shortly after the first oligothiophene-based SMBHJs. Roncali and co-workers reported a series of triphenylamine-thiophene-acceptor structures only months after reporting the first oligothiophene SMBHJ.<sup>44–46</sup> Increasing the number of electron withdrawing groups in this series of compounds caused a deepening of the HOMO energy level and a decrease in the band gap with a concomitant increase in  $V_{OC}$  and  $J_{SC}$ . The most effective material (structure **13**) reported in SMBHJ devices with PCBM showed an absorption onset of 680 nm in the solid state and yielded devices with a  $J_{SC}$  of 4.1 mA/cm<sup>2</sup>,  $V_{OC}$  of 0.66 V, FF of 0.30, and PCE of 0.81%.

In 2007, Zhou et al. reported pull-push–pull chromophores based on carbazole or phenothiazine as a push moiety and 3-(1,3-dithiolan-2-yl)pentane-2,4-dione or 2-(5,5-dimethylcyclohex-2-enylidene)malononitrile as pull moiety (structure **14**). Stronger electron-donating ability was observed from phenothiazine, evidenced by red-shifted intramolecular charge transfer absorption band. Adversely, the HOMO was destabilized, reducing  $V_{OC}$  from 0.7 to 0.5 V. When incorporated in solar cell devices, the compound with malononitrile and carbazole yielded a PCE of 0.51%.<sup>47</sup>

Li and co-workers reported a series of triphenylamine based push–pull chromophores with benzothiadiazole (BT) or dicyanomethene pull moieties.<sup>48–52</sup> An unusually high  $V_{OC}$  of 1.21 V was observed using the benzothiadiazole-based material as an acceptor,<sup>49</sup> whereas a  $V_{OC}$  of 0.87 V was achieved by using PCBM as an acceptor.

Later, they observed that a star-shaped material performed better than the linear shaped material, i.e., PCE of 1.33% with S(TPA-BT) versus PCE of 0.35%.<sup>50</sup> Devices using the star-shaped material were further improved to 2.39% by using PC<sub>71</sub>BM as an electron acceptor and replacing the end group of triphenylamine in S(TPA-BT) with 4-hexylthiophene (structure **15**), which increased absorption at the band maximum to 529 nm.<sup>52</sup>

In 2008, Cao and co-workers reported another TPA-BT system with a thienyl fluorene bridge.<sup>53</sup> SMBHJs from this material were modestly efficient, exhibiting a  $J_{SC}$  of 1.59 mA/cm<sup>2</sup>, a  $V_{OC}$  of 0.70 V, FF of 0.22, and PCE of 0.22%.

Also in 2008, Lincker et al. published a report describing a chromophore consisting of a central fluorenone pull moiety between two tetrathiophene oligomers,<sup>54</sup> yielding optimized devices with a  $J_{SC}$  of 3.61 mA/cm<sup>2</sup>, a  $V_{OC}$  of 0.82 V, FF of 0.40, and PCE of 1.19%.

A topologically simple push–pull system was reported by Wong and co-workers<sup>55</sup> involving a triarylamine “push” unit and dicyanovinyl “pull” group with an oligothiophene bridge of varying length. This type of molecule was first demonstrated in a solution processed donor/evaporated C<sub>60</sub> bilayer and then in a BHJ type cell.<sup>56</sup> The best performing material (structure **16**) in this study exhibited a HOMO of 5.1 eV, a LUMO of 3.36 eV and yielded optimized devices with a  $J_{SC}$  of 5.41 mA/cm<sup>2</sup>,  $V_{OC}$  of 0.79 V, FF of 0.40, and PCE of 1.72%.

Xue et al. were able to double the performance of a SMBHJ system by reducing the size of the molecule, comparing 2-{2,6-bis-[2-(4-diphenylamino-phenyl)-vinyl]-pyran-4-ylidene}-malononitrile (DADP) and triphenylamine-dicyanomethane-triphenylamine (TPA-DCM-TPA).<sup>57</sup> Decreasing the distance between push and pull moieties by removing phenylene vinylene stabilized the HOMO and

Table 4. Structures and Electronic Properties of Several Push-Pull Type Chromophores

architecture	push moiety	$\pi$ -bridge	pull moiety	HOMO (eV)	LUMO (eV)	optim. Voc (V)	film abs. onset (nm)	optim. Jsc (mA/cm <sup>2</sup> )	optim. PCE (%)	ref.
	triphenylamine	thienovinyliothiophene	indanedione	---	---	0.66	680 <sup>a</sup>	4.10	0.81	44
	carbazole	diene	dicyanovinyl	5.47	3.42	0.72	600	2.2	0.51	47
	triphenylamine	divinylbenzene	pyranylidene-malonitrile	5.14	2.76	0.90	620	2.14	0.79	48
	triphenylamine	vinyl	benzothiadiazole	5.30	3.27	0.81	640	4.18	1.33	50
	triphenylamine	divinylbenzene	pyranylidene-malonitrile	5.28	3.47	0.77	630	2.37	0.73	51
	triphenylamine	vinyl	benzothiadiazole	5.19	3.08	0.85	630	8.58	2.39	52
	triphenylamine	thienylfluorene	benzothiadiazole	5.30	3.41	0.70	630	1.59	0.22	53
	tetra-thiophene	---	fluorenone	5.16	3.25	0.82	650	3.61	1.19	54
	diphenylfluorenylamine	pentathiophene	dicyanovinyl	5.10	3.36	0.79	680 <sup>a</sup>	5.41	1.72	56
	triphenylamine	vinyl	pyranylidene-malonitrile	5.28	3.45	0.98	610	4.16	1.50	57
	triphenylamine	thiophene	benzothiadiazole	5.4	3.3	0.92	590	4.9	1.8	58
	triphenylamine	vinyl	benzothiadiazole	5.27	3.10	0.96	620	5.50	1.96	59
	triphenylamine	thiophene	benzothiadiazole	5.16	2.99	0.86	630	3.5	1.23	60
	heptathiophene	---	dicyanovinyl	5.13	3.42	0.88	750	12.4	3.7	62

All abs. onsets were estimated by finding the intercept of the line tangent to the inflection point of the absorption onset and the line defined by the baseline data at the red end of the spectrum. <sup>a</sup>Where thin film absorption data were not available, absorption onsets were estimated from EQE data.

LUMO energy levels from 5.14 and 2.76 eV to 5.28 and 3.45 eV, respectively, while enhancing charge mobility from  $1.19 \times 10^{-6}$  to  $1.38 \times 10^{-5}$  cm<sup>2</sup>/(V s) as measured using single-carrier diodes. As a result, a larger  $J_{SC}$ ,  $V_{OC}$ , and higher PCE (4.16 mA/cm<sup>2</sup>, 0.98 V, and 1.5% versus 2.02 mA/cm<sup>2</sup>, 0.75 V, and 0.6%, respectively) were achieved.

Bo and co-workers first demonstrated a series of star-shaped molecules based on multifunctionalized benzothiadiazole core.<sup>58</sup> Interestingly, the star-shaped molecules exhibited deeper HOMO and wider band gap than corresponding linear molecules. The best star-shaped molecule with PCBM device produced a  $V_{OC}$  of 0.92 V,  $J_{SC}$  of 4.9 mA/cm<sup>2</sup>, FF of 0.41, and PCE of 1.8%.

Yang et al. reported a small molecule with a triphenylamine core and two arms of benzothiadiazole-hexylthiophene yielding  $J_{SC}$  of 5.50 mA/cm<sup>2</sup>,  $V_{OC}$  of 0.96 V, FF of 0.37, and PCE of 1.96%.<sup>59</sup> Shang et al. reported a benzothiadiazole core thiophene-bridged to triphenylamine

small molecule yielding a  $J_{SC}$  of 3.50 mA/cm<sup>2</sup>,  $V_{OC}$  of 0.86 V, FF of 0.41, and PCE of 1.23%.<sup>60</sup>

One interesting result was recently obtained by Liu et al. by terminating an oligothiophene with dicyanovinyl moieties (structure 17). The terminal electron-withdrawing groups narrowed the band gap of the heptathiophene, extending the absorption to 750 nm. This broad absorption, coupled with a relatively high hole mobility of  $1.5 \times 10^{-4}$  cm<sup>2</sup>/(V s), allowed this system to produce an unusually large current. The optimized device produced a  $J_{SC}$  of 12.4 mA/cm<sup>2</sup>,  $V_{OC}$  of 0.88 V, FF of 0.4, and PCE of 3.7%.<sup>61,62</sup>

In the case of push-pull chromophores, it appears that more complicated molecules are not necessarily better; relatively high efficiencies can be obtained using a simple push- $\pi$ -pull architecture, or even a simple oligothiophene with pull moieties. In contrast to pure oligothiophenes, which keep improving with size, push-pull



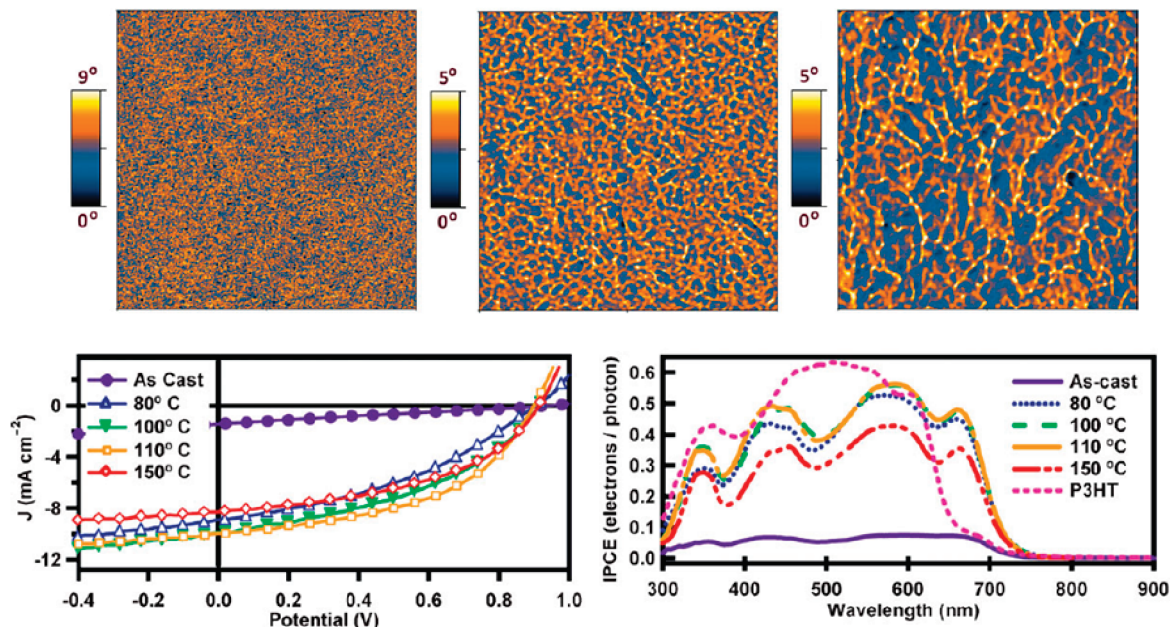


**Figure 5.** AFM phase images (top) of SMBHJs comprising **20** and PC<sub>71</sub>BM as-cast (left), annealed at 90 °C (middle), and 100 °C (right), showing that the phase separation domain size can be controlled by changing the annealing temperature. Images are 2  $\mu\text{m} \times 2 \mu\text{m}$ . Current–voltage curves (lower left) show that optimum device characteristics are obtained after annealing at 110 °C. EQE spectra (lower right) show that high photocurrent generation ( $>40\%$  photons  $\rightarrow$  electrons) occurs throughout the visible spectrum from 400 to 700 nm. This spectrum compares favorably to and integrates to larger currents than devices based on the well-known polymer P3HT. Reproduced with permission from ref 5. Copyright 2009 Wiley-VCH Verlag GmbH & Co. KGaA.

oligomers lengths may have finite optimum values, because of decreased electronic communication between push and pull moieties. It is also apparent that desirable HOMO and LUMO values can be obtained by coupling a wide variety of electron donating and withdrawing moieties. Table 4 highlights the structures and optoelectronic properties of some of most successful push–pull materials discovered by various groups.

### Diketopyrrolopyrroles

Motivated by the synthetic reproducibility of small molecules, our group began studying molecular donor materials by using the 3,6-diaryl-2,5-dihydro-pyrrolo-[3,4-c]pyrrole-1,4-dione (DPP) architecture, a type of molecule used in high-performance pigments for industrial applications.<sup>63,64</sup> Several aspects of industrial pigments, such as strong light absorption, photochemical stability, and large-scale synthesis make them promising for solar cell applications.<sup>65</sup> Among them, DPP is an attractive building block in terms of facile synthetic modification, i.e., alkyl substitution on 3,4-position (nitrogen on the lactam) and substitution of various aromatic groups on the 2,5-positions. Our group has demonstrated that molecular packing in the solid state and optical properties can be controlled by these substituents.<sup>66</sup> For instance, by adding oligothiophenes of increasing length to the 3, 6 positions on the DPP core, the absorption is broadened while the band gap is decreased, yielding materials that have a tendency to self-assemble into ordered structures upon thermal annealing and exhibit field-effect mobilities of up to 0.01  $\text{cm}^2/(\text{V s})$ <sup>67</sup>—attractive properties for solar cell applications.

The first soluble DPP-based oligothiophene we explored (structure **18**) as a SMBHJ material with PCBM achieved a  $J_{\text{SC}}$  of 8.42  $\text{mA}/\text{cm}^2$ ,  $V_{\text{OC}}$  of 0.67, FF of 0.45, and a relatively high PCE of 2.3%, the highest SMBHJ solar cell performance at that time. However, the material carried potential morphological instability due to thermally labile alkyl group, i.e., the *t*-Boc, on 2,5-positions.<sup>68</sup> By replacing the *t*-Boc substituent with the ethylhexyl group (structure **19**), morphological and thermal stability were improved. The HOMO and LUMO were changed from 4.9 to 5.2 eV and from 3.4 to 3.7 eV, respectively, as measured by UPS. In addition, intermolecular interaction in the blend with PCBM was also improved, as evidenced by the extension of absorption to longer wavelengths. While the compound with *t*-Boc showed an imbalance of carrier mobilities by 3 orders of magnitude (hole mobility of  $5 \times 10^{-7} \text{cm}^2/(\text{V s})$  and electron mobility of  $3 \times 10^{-4} \text{cm}^2/(\text{V s})$  as measured using single-carrier diodes), the ethylhexyl DPP derivative displayed balanced carrier mobilities when blended with PCBM, i.e., hole mobility of  $1.0 \times 10^{-4} \text{cm}^2/(\text{V s})$  and electron mobility of  $4.8 \times 10^{-4} \text{cm}^2/(\text{V s})$ . These improvements resulted in solar cells achieving a  $J_{\text{SC}}$  of 9.2  $\text{mA}/\text{cm}^2$ ,  $V_{\text{OC}}$  of 0.75, FF of 0.44, and PCE of 3.0%.<sup>69</sup> Structure **19** was also blended with P3HT:PC<sub>71</sub>BM active layer at a small weight percent ( $\sim 2\%$  by weight) to extend the absorption and photocurrent to 800 nm.<sup>70</sup>

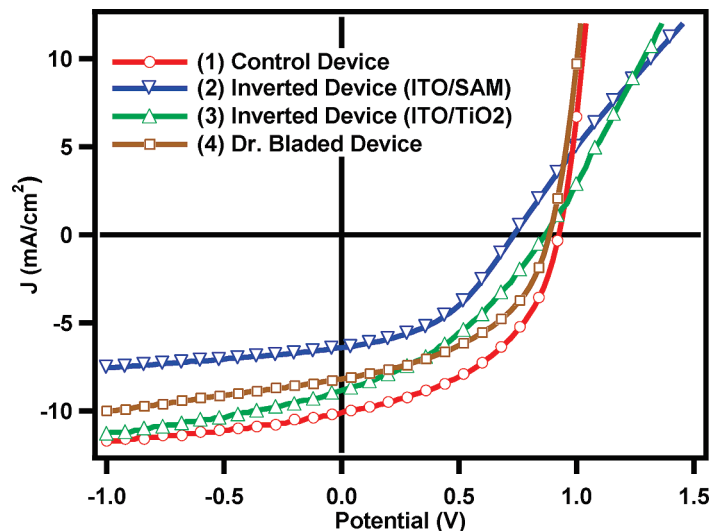
The solar cell performance of DPP-based materials was further improved by replacing terminal bithiophene with benzofuran (structure **20**).<sup>5</sup> The benzofuran substituent increases intermolecular chromophore interaction through the high conjugation and stabilizes the molecules HOMO due to the electronegative oxygen atom. This



Table 5. Optimum Results Based on First Three Published DPP-Based Molecular Donors

donor structure	acceptor	D:A ratio	donor MW (Da)	abs. onset (nm)	hole mobility <sup>a</sup> (cm <sup>2</sup> /(V s))	$J_{sc}$ (mA/cm <sup>2</sup> )	$V_{oc}$ (V)	FF (%)	PCE (%)	ref
18	PC <sub>61</sub> BM	7:3	997	800	$5 \times 10^{-7}$	8.42	0.67	45	2.3	68
19	PC <sub>71</sub> BM	1:1	1022	800	$1.0 \times 10^{-4}$	9.2	0.75	44	3.0	69
20	PC <sub>71</sub> BM	6:4	757	710	$3.0 \times 10^{-5}$	10	0.92	48	4.4	5

<sup>a</sup> Space charge limited current mobility for optimized blend with fullerene acceptor.



device	1	2	3	4
$J_{sc}$ (mA/cm <sup>2</sup> )	10.13	6.41	8.84	8.19
$V_{oc}$ (V)	0.93	0.73	0.87	0.89
FF	0.47	0.43	0.37	0.46
$\eta$ (%)	4.39	2.05	2.81	3.34
$R_{series}$ ( $\Omega$ )	13.0	312.7	307.6	22.8
$R_{parallel}$ (k $\Omega$ )	3,733	15	38	6

**Figure 6.**  $J$ – $V$  characteristics of devices prepared by nonconventional techniques compared to a conventional device. Device 1 is a conventional device prepared using the architecture ITO/PEDOT/DPP(TBFu)<sub>2</sub>:PC<sub>71</sub>BM/Al. Device 2 was prepared using the architecture ITO/SAM/DPP(TBFu)<sub>2</sub>:PC<sub>71</sub>BM/PEDOT:PSS/Au, where PEDOT:PSS was deposited by mixing an H. C. Stark Clevis P VP 4083 dispersion with 2 volumes of isopropanol and spincoating at 2500 rpm. Device 3 was prepared using the architecture ITO/TiO<sub>2</sub>/DPP(TBFu)<sub>2</sub>:PC<sub>71</sub>BM/PEDOT:PSS/Au, where the TiO<sub>2</sub> layer was prepared by spincoating a 4% solution of titanium isopropoxide from a mixed solvent consisting of 1:9 dimethoxyethane:isopropanol at 3000 rpm in an atmosphere containing 20 ppm H<sub>2</sub>O followed by annealing at 300 °C for 30 min and PEDOT:PSS was deposited as in device 2. Device 4 has the same architecture as Device 1 but the active layer was deposited by doctor-blading in air.

material exhibits a HOMO of 5.2 eV and LUMO of 3.4 eV as measured by UPS. When blended with PC<sub>71</sub>BM, very little phase separation is apparent in the as-cast films. However, upon thermal annealing, the surface of the film roughens and shows distinct donor and acceptor domains which increase in size with increasing annealing temperatures from 80 °C – 180 °C (Figure 5); thus, the degree of phase separation can be controlled by the annealing temperature, with 110 °C yielding optimum device properties. The deep HOMO band in this material yields an increased  $V_{oc}$  of 0.9 V or more, a  $J_{sc}$  of 10 mA/cm<sup>2</sup>, FF of 0.48, an optimized device efficiency of 4.4%, and an EQE reaching 58% in the 600 nm region (Figure 5).<sup>5</sup> Table 5 summarizes the results obtained with the first three DPP SMBHJs.

Initially, our group studied dithienodPP-based materials, in which the 3,6-position of DPP is linked to thiophene groups. Recently, we have expanded our study to diphenyl DPP-based materials (structure **21**) to understand the effect of structural variation on solid-state electronic properties relevant to device performance.<sup>71</sup> Drastic effects of structural variation on electronic properties were observed by film characterization. Only conjugation length determines the band gap in solution; however, optical band gap in the solid state is affected by conjugation length as well as alkyl substitution, which modifies the aggregation/molecular packing in the solid state. This observation emphasizes the importance of controlling molecular packing in the solid state.

We have found that the  $V_{oc}$  of DPP SMBHJs can be increased by changing the acceptor, such as using fullerenes with large alkyl substituents,<sup>72</sup> or by using acceptors with higher lying LUMO levels such as vinazene type compounds.<sup>73–76</sup> Unfortunately, this increase in  $V_{oc}$  (for instance, from 0.92 to 1.24 V changing from PCBM to a vinazene type acceptor<sup>77</sup>) is typically accompanied by a decrease in  $J_{sc}$  (which drops from 10 to about 2 mA/cm<sup>2</sup> using vinazene).

To manufacture organic solar cells on a larger scale, flexibility in the fabrication and architecture of the system is of great interest. For instance, the ability to deposit active layers by doctor-blading is appealing for the production of large area solar cells, while the ability to fabricate inverted devices using a variety of substrates and stable electrodes such as metal oxides and high work function metals is also appealing. We have found that DPP materials can be deposited by doctor blading technique (albeit with some decrease in efficiency) and can also be processed on metal oxides substrates such as ZnO or TiO<sub>2</sub> to give inverted devices (also with a decrease in efficiency). Figure 6 compares  $J$ – $V$  curves of devices prepared using spin-casted inverted structures (ITO/SAM or TiO<sub>2</sub>/active layer/PEDOT:PSS/Au) against spin-cast and doctor bladed standard devices (ITO/PEDOT:PSS/active layer/Al). SAM refers to a self-assembled monolayer of 3-aminopropyltriethoxysilane that has been shown to

modify the ITO surface to reduce its work function from 4.7 to 4.3 eV.<sup>78</sup>

Although all of DPP-based small molecules discussed so far have been used as electron donors in BHJ solar cells, Sonar and co-workers demonstrated the use of a DPP-based material as an electron acceptor by incorporating aromatic moiety with electron-withdrawing group on 2,5-position on DPP.<sup>79</sup> Using one of the DPP derivatives whose HOMO, LUMO, and optical band gap are 5.26, 3.52, and 1.94 eV, respectively, a device with an active layer containing P3HT:DPP exhibited a  $J_{SC}$  of 2.36 mA/cm<sup>2</sup>,  $V_{OC}$  of 0.81 V, a FF of 0.52, and PCE of 1.0%.

Recently, Janssen and co-workers synthesized triads consisting of a DPP core covalently bonded to two fullerene groups to study the photophysics and energy transfer processes of the DPP system by transient absorption.<sup>80</sup> Upon photoexcitation, ultrafast energy transfer to the fullerene was found to occur on a time scale of 0.5 ps, followed by charge separation with a time constant of 18–47 ps and recombination with a constant of 37–500 ps. The authors concluded that 14% of the charge recombination occurred via a DPP triplet state. Devices based on this material have not been reported.

### Dyes and Other Materials

A variety of other materials have appeared in the literature over the past few years incorporating a diverse assortment of structures, including several well-known classes of dye molecules such as borondipyrromethene (BODIPY),<sup>81–83</sup> merocyanine,<sup>84,85</sup> squaraine,<sup>86–89</sup> isoindigo,<sup>90</sup> and phthalocyanine.<sup>12,91,92</sup> As several groups have demonstrated, functionalizing a dye molecule with solubilizing groups has proven to be a successful approach to SMBHJ donor design.

Recently, Roncali and co-workers have shifted focus from oligothiophenes to chromophores of the BODIPY structure. This type of dye can be used as a platform for the design of donor materials which exhibit outstanding absorption coefficients of up to 126 000 M<sup>-1</sup> cm<sup>-1</sup>.<sup>81</sup> By combining two of these BODIPY dyes with complementary absorption characteristics and blending with PCBM, Roncali's group has been able to fabricate devices showing EQE of greater than 20% from 400 to 700 nm yielding a  $J_{SC}$  of 4.7 mA/cm<sup>2</sup>,  $V_{OC}$  of 0.87 V, FF of 0.42, and PCE of 1.7%.<sup>82</sup> Considering that the phenyl group on BODIPY is not coplanar, bithiophene was incorporated on the first BODIPY derivative to give structure **22**, resulting in increased hole mobility and broadened absorption while retaining the electronic and optical properties of BODIPY.<sup>83</sup> The crystallinity was slightly improved and the hole mobility increased from  $5 \times 10^{-5}$  cm<sup>2</sup>/(V s) to  $9.7 \times 10^{-5}$  cm<sup>2</sup>/(V s), leading to a  $J_{SC}$  of 7.0 mA/cm<sup>2</sup>,  $V_{OC}$  of 0.75 V, FF of 0.38, and PCE of 2.2%.

Meerholz and co-workers have demonstrated the viability of the merocyanine (MC) class of chromophore in BHJ devices. After identifying a promising structure through the analysis of seven different MC homologues,<sup>84</sup> they modified

the structure by covalently bonding the alkyl chain on pyrrole moiety to the adjacent benzene ring (structure **23**), in order to control molecular packing in the solid state by rigidification. Interestingly, while the original compound showed a drop in hole mobility upon mixing with PCBM by 2 orders of magnitude, the hole mobility of **23** decreases only slightly upon blending with PCBM. Increased crystallinity, as observed by thin film X-ray diffraction (XRD), enhanced charge transport and photocurrent, improved the PCE from 1.54% to 2.59%.<sup>85</sup>

Squaraine is a promising class of dye for BHJ solar cells because it strongly absorbs the light over a broad range from 500 to 900 nm and possesses photochemical and thermal stability. Pagani and co-workers reported  $J_{SC}$  of 5.70 mA/cm<sup>2</sup>,  $V_{OC}$  of 0.62 V, FF of 0.35, and PCE of 1.24% from devices processed in the air.<sup>86</sup> The authors reported PCEs of up to 2.05% using the same conjugated structure with hexenyl solubilizing groups (structure **24**).<sup>87</sup>

Wurthner and co-workers reported an unusually high  $J_{SC}$  of up to 12.6 mA/cm<sup>2</sup> from their squaraine-based small molecule (structure **25**) with PCBM.<sup>88</sup> Crystallinity was increased by replacing the ketone on the squaraine moiety with dicyanovinyl group (structure **25**), resulting in a hole mobility of up to  $1.3 \times 10^{-3}$  cm<sup>2</sup>/(V s) and a high FF of 0.47. However, the  $V_{OC}$  of 0.31 V was rather low. Wei et al. also recently reported a squaraine (structure **26**) SMBHJ using PCBM as an acceptor. These devices achieved a  $J_{SC}$  of 8.85 mA/cm<sup>2</sup>,  $V_{OC}$  of 0.89 V, FF of 0.35, and PCE of 2.7%. The PCE was improved to 2.9% by adding an evaporated BCP layer at the cathode. In this study, bilayer control devices using the same donor material with evaporated C<sub>60</sub> layers were found to have a significantly higher PCE of 4.1%, largely due to a higher FF of 0.54.<sup>89</sup>

In addition to DPP and MC, indigo derivatives are among the well-known industrial dyes, and have been employed as a building block in BHJ solar cell materials. Reynolds et al. reported two types of isoindigo based oligothiophenes: donor–acceptor–donor (D–A–D, structure **27**) and acceptor–donor–acceptor (A–D–A). Interestingly, two molecules show very similar energy levels. The same HOMO of 5.5 eV was observed for both and LUMO of 3.9 and 3.8 eV for D–A–D and A–D–A, respectively, were observed. When blended with PCBM and annealed, more crystalline domains were observed from the blend of D–A–D and PCBM, than A–D–A, as revealed by AFM images. This might be the reason for higher performance observed in the D–A–D structure. D–A–D and A–D–A devices prepared in this manner yielded  $J_{SC}$ 's of 6.3 and 2.4 mA/cm<sup>2</sup>,  $V_{OC}$ 's of 0.74 and 0.66 V, FF's of 0.38 and 0.36, and PCE's of 1.76 and 0.55%, respectively.<sup>90</sup>

Frechet's group reported a series of platinum-acetylide oligomers, in which intramolecular charge transfer (ICT) chromophore were confined with platinum-acetylide on both sides, and various oligothiophenes were connected to control the molecular packing by changing the number of thiophene units from two to four. While absorption at short wavelength increased with the length of oligothiophene,

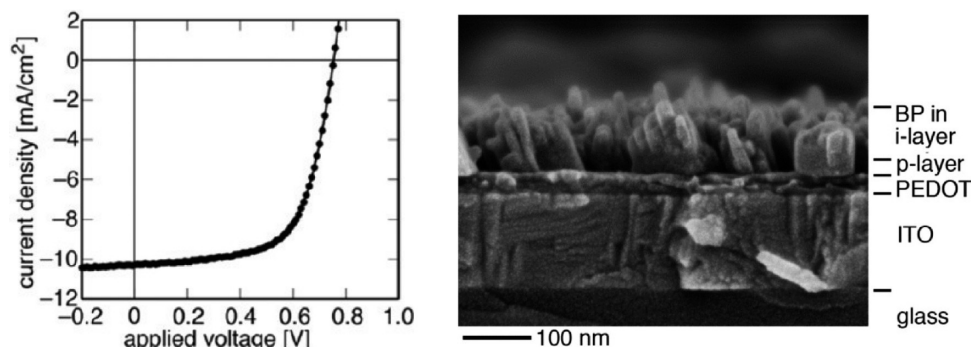


**Figure 7.**  $J$ - $V$  characteristics and cross-sectional SEM image of Matsuo's solution processed bilayer device. The device was prepared by spin-casting a precursor solution atop the PEDOT:PSS layer followed by thermal annealing at 180 °C to convert to tetrabenzoporphyrin (BP, p-layer). Subsequently, a soluble BP precursor and bis(dimethylphenylsilylmethyl)[60]fullerene (SIMEF) solution was spun atop the pure BP layer (i-layer) and followed by a pure layer of SIMEF (n-layer) and Al deposition. Reproduced with permission from ref 92. Copyright 2009 American Chemical Society.

**Table 6. Comparison of Material Properties and Device Characteristics Using Miscellaneous Dye-Based Donor Materials**

donor structure	acceptor	D:A ratio	donor MW (Da)	abs. onset (nm)	hole mobility ( $\text{cm}^2/(\text{V s})$ )	$J_{\text{sc}}$ ( $\text{mA}/\text{cm}^2$ )	$V_{\text{oc}}$ (V)	FF (%)	PCE (%)	ref
22	PC <sub>61</sub> BM	1:2	1145	720	$9.7 \times 10^{-5a}$	7	0.75	38	2.17	83
23	PC <sub>61</sub> BM	9:11	403	700	$2.0 \times 10^{-5b}$	8.24	0.94	34	2.59	85
24	PC <sub>71</sub> BM	1:3	797	850	$1 \times 10^{-4}$ to $1 \times 10^{-5c}$	9.32	0.57	37	1.99	87
25	PC <sub>61</sub> BM	6:4	537	900	$1.3 \times 10^{-3c}$	12.6	0.31	47	1.79	88
26	PC <sub>71</sub> BM	1:6	553	750	$1.2 \times 10^{-7d}$	8.85	0.89	35	2.7	89
27	PC <sub>61</sub> BM	1:1	984	740		6.3	0.74	38	1.76	90
28	PC <sub>71</sub> BM	1:4	1752	650	$1 \times 10^{-4}$ to $1 \times 10^{-5d}$	8.45	0.82	43	3.0	93
29	30	1:1	652	750	$1.3 \times 10^{-4d}$	8.3	0.90	52	3.88	95
Mixture	31	7:3	800–3800	850		1.24	0.41	24	0.12	91
32	33		511	710		10.5	0.75	65	5.2	92

<sup>a</sup> Space charge limited current mobility measured for neat film. <sup>b</sup> Field effect mobility measured for blend film. <sup>c</sup> Field effect mobility measured for neat film. <sup>d</sup> Space charge limited current mobility measured for for blend film.

absorption of ICT band and energy levels were not affected by the length of oligothiophenes. As a result, all the molecules showed same HOMO and LUMO i.e., 5.3 and 3.4 eV, respectively. It seems that longer oligothiophene was detrimental to the hole mobility. As the length of thiophene increased from two to four, hole mobility decreased from  $2.7 \times 10^{-4} \text{ cm}^2/(\text{V s})$  to  $0.9 \times 10^{-4} \text{ cm}^2/(\text{V s})$ . Blended with PC<sub>71</sub>BM, the oligomer with terthiophene (structure **28**) produced the best device performance, showing a  $J_{\text{SC}}$  of 8.45 mA/cm<sup>2</sup>,  $V_{\text{OC}}$  of 0.82 V, FF of 0.43, and PCE of 3.0%.<sup>93</sup>

Mikroyannidis et al. recently reported an unprecedentedly high efficiency using a non-fullerene acceptor. An efficiency of 3.88%, combined with  $J_{\text{SC}}$  of 8.30 mA/cm<sup>2</sup>,  $V_{\text{OC}}$  of 0.90 V, and FF of 0.52, were achieved using a SMBHJ system involving a donor containing nitrophenyl, cyanovinyl, thiophene and benzoselenadiazole moieties (structure **29**) with a perylene bisimide acceptor (structure **30**).<sup>94,95</sup> Upon annealing the blended film, the hole mobility increased from  $3.4 \times 10^{-5} \text{ cm}^2/(\text{V s})$  to  $1.3 \times 10^{-4} \text{ cm}^2/(\text{V s})$ , whereas noticeable change in electron mobility was not observed, i.e., from  $4.6 \times 10^{-4} \text{ cm}^2/(\text{V s})$  to  $5.1 \times 10^{-4} \text{ cm}^2/(\text{V s})$ . In addition, increase in crystallinity of the annealed blend film was observed by topographic optical image and XRD.

The very first reported SMBHJs involved phthalocyanines and although these first devices might not have been very efficient, recent work has shown that phthalocyanines are a viable donor for use in SMBHJs. In a recent report by Varotto et al., significantly improved

performance was realized by using a combination of three phthalocyanine donors and a fullerene acceptor (structure **31**) to give devices with a  $J_{\text{SC}}$  of 1.24 mA/cm<sup>2</sup>,  $V_{\text{OC}}$  of 0.41 V, FF of 24%, and PCE of 0.12%.<sup>91</sup>

Although perhaps more of an “ordered” heterojunction than BHJ, Nakamura and co-workers have fabricated very nice photovoltaics by sequentially depositing a thermally transformable phthalocyanine (structure **32**) and silyl fullerene derivative (structure **33**) from solution. Trilayer device structures were used with a pure donor layer (p-layer), a BHJ layer (i-layer), and a pure acceptor layer (n-layer). The trilayer devices exhibit some of the largest  $J_{\text{SC}}$  (10.3 mA/cm<sup>2</sup>) and FF (65%) reported for solution-processed small molecule solar cells, leading to an impressive overall PCE of 5.2%. The high efficiency is due to the formation of crystalline columnar benzoporphyrin nanostructures as seen in the scanning electron microscopy (SEM) image of the device cross section (Figure 7, right).

It is evident from these reports that using organic dye molecules as platforms for the design of SMBHJs is an effective strategy. Table 6 compares the results for optimized systems using organic chromophores as donor materials.

## Conclusions

A great variety of molecular heterojunction materials have been reported over the past several years and it is evident that most of the design principles that apply to



polymer solar cells<sup>96</sup> in terms of energy levels and device properties also apply to SMBHJs. It has been demonstrated that the absorption characteristics, energy levels, and even charge-carrier mobilities can be controlled fairly well through the careful design of small molecules and can lead to materials with desirable optoelectronic properties, often matching those of the most efficient conjugated polymer systems.

A few conclusions can be made about individual classes of materials. Oligothiophenes seem to improve with increasing conjugation length and molecular weight, but it seems unlikely that they will outperform P3HT. As such, they make an interesting model system to study. Soluble acenes show great promise as materials with high carrier mobilities, where relatively low band gaps can be achieved using compact structures. It has been demonstrated that solublizing groups allow good control over their solid structure. Acenes that produce films with smaller feature sizes tend to produce larger current densities and better results. As with polymers, push–pull design strategies are an effective way to produce molecular donors with broad absorption and fine-tuned energy levels. Finally, structures that are well-known as pigments and dyes have shown great promise as light-harvesting donor materials in SMBHJs. For example, the DPP chromophore unit has proven to be a versatile platform for the design of solar cell materials. Functionalization of the lactam nitrogens with solublizing groups enables materials to be solution processed, whereas substitution of the 3,6 positions with aryl groups leads to compounds with broad absorption and energy levels which are well-aligned with those of PCBM. These relatively compact structures involve a few straightforward synthetic steps and show promise as mass-producible materials for next-generation solar cells.

As a general trend with most of the SMBHJ materials discussed in this review, the  $V_{OC}$  tends to be higher than that observed in analogous polymer devices, while the FF and  $J_{SC}$  of SMBHJs are usually considerably lower. Examining the light versus dark curves for most of the devices shows that in almost all cases, the photocurrent produced by SMBHJs becomes significantly larger at reverse bias. These points seem to imply that carrier extraction and recombination limit current generation in these SMBHJs much more than is the case in polymer based BHJs. This trend could be explained in terms of the morphology of molecular heterojunctions, where small molecules tend to result in morphologies with more charge-trapping “cul-de-sacs” and dead ends, whereas higher-molecular-weight polymers more readily form percolated networks with continuous carrier transport pathways to electrodes. Unfortunately, this hypothesis is difficult to verify directly because of the difficulty and limitation of characterization methods to analyze the cross-sectional composition of such films. However, the point can be rationalized by comparing molecular bilayer heterojunctions to molecular bulk heterojunctions. Bilayers have continuous pathways for carrier transport, exhibit photocurrents which saturate at relatively small

electric fields, and show high FFs (though the reduced D–A interfacial area tends to result in smaller  $J_{SC}$ ). Matsuo’s results with a structured heterojunction seem to support this view as well, as his architecture incorporated a large interfacial area with “forced” percolation pathways, which resulted in a large current density and one of the highest fill factors observed for a solution processed molecular heterojunction.

The next big challenge in SMBHJs may be finding strategies to control the morphology to maximize D–A interfacial area while minimizing structurally induced recombination losses; allowing for large short circuit currents and high fill factors in SMBHJs, such as those demonstrated in Matsuo’s junction. It is not unlikely that molecules exist which are able to spontaneously form such films. As of now, the range of solublizing groups explored in SMBHJ materials has been limited to a handful hydrocarbon and alkylsilyl groups and this presents a potentially fruitful area of study. The ability to fine-tune the phase separation and self-assembly of molecular solids via synthetic design may put them in a position to compete with polymers as the preferred type of organic semiconductor for high efficiency solar cells.

**Acknowledgment.** The authors are grateful for the financial support from the Office of Naval Research and the Department of Energy, Basic Science Research. B.W. gratefully acknowledges support from the ConvEne IGERT Program (NSF-DGE 0801627).

**Note Added after ASAP Publication.** There were several errors in the version published ASAP November 4, 2010; the corrected version was published ASAP December 16, 2010.

## References

- (1) Dennler, G.; Scharber, M. C.; Brabec, C. J. *Adv. Mater.* **2009**, *21*, 1323.
- (2) Chen, H.-Y.; Hou, J.; Zhang, S.; Liang, Y.; Yang, G.; Yang, Y.; Yu, L.; Wu, Y.; Li, G. *Nat. Photonics* **2009**, *3*, 649.
- (3) Hummelen, J. C.; Knight, B. W.; Lepeq, F.; Wudl, F.; Yao, J.; Wilkins, C. L. *J. Org. Chem.* **1995**, *60*, 532.
- (4) In this review, SMBHJs are defined as solar cells incorporating a solution-processed active layer comprising donor and acceptor organic semiconductors that both have discrete (nonpolymeric) molecular structures.
- (5) Walker, B.; Tamayo, A. B.; Dang, X. D.; Zalar, P.; Seo, J. H.; Garcia, A.; Tantiwatt, M.; Nguyen, T.-Q. *Adv. Funct. Mater.* **2009**, *19*, 3063.
- (6) Li, G.; Shrotriya, V.; Huang, J.; Yao, Y.; Moriarty, T.; Emery, K.; Yang, Y. *Nat. Mater.* **2005**, *4*, 864.
- (7) Ma, W.; Yang, C.; Gong, X.; Lee, K.; Heeger, A. J. *Adv. Funct. Mater.* **2005**, *15*, 1617.
- (8) Lloyd, M. T.; Anthony, J. E.; Malliaras, G. G. *Mater. Today* **2007**, *10*, 34.
- (9) Roncali, J. *Acc. Chem. Res.* **2009**, *42*, 1719.
- (10) Halls, J. J. M.; Walsh, C. A.; Greenham, N. C.; Marseglia, E. A.; Friend, R. H.; Moratti, S. C.; Holmes, A. B. *Nature* **1995**, *376*, 498.
- (11) Yu, G.; Gao, J.; Hummelen, J. C.; Wudl, F.; Heeger, A. J. *Science* **1995**, *270*, 1789.
- (12) Petritsch, K.; Dittmer, J. J.; Marseglia, E. A.; Friend, R. H.; Lux, A.; Rozenberg, G. G.; Moratti, S. C.; Holmes, A. B. *Sol. Energy. Mater. Sol. Cells* **2000**, *61*, 63.
- (13) Schmidt-Mende, L.; Fechtenkotter, A.; Mullen, K.; Moons, E.; Friend, R. H.; MacKenzie, J. D. *Science* **2001**, *293*, 1119.
- (14) Schmidt-Mende, L.; Fechtenkotter, A.; Mullen, K.; Friend, R. H.; MacKenzie, J. D. *Physica E* **2002**, *14*, 263.
- (15) Van de Craats, A. M.; Warman, J. M. *Adv. Mater.* **2001**, *13*, 130.
- (16) Roncali, J.; Frere, P.; Blanchard, P.; De Bettignies, R.; Turbiez, M.; Roquet, S.; Leriche, P.; Nicolas, Y. *Thin Sol. Films* **2006**, *511*, 567.
- (17) Sun, X.; Zhou, Y.; Wu, W.; Liu, Y.; Tian, W.; Yu, G.; Qiu, W.; Chen, S.; Zhu, D. *J. Phys. Chem. B* **2006**, *110*, 7702.

- (18) Lloyd, M. T.; Mayer, A. C.; Tayi, A. S.; Bowen, A. M.; Kasen, T. G.; Herman, D. J.; Mourey, D. A.; Anthony, J. E.; Malliaras, G. G. *Org. Electron.* **2006**, *7*, 243.
- (19) Karpe, S.; Cravino, A.; Frère, P.; Allain, M.; Mabon, G.; Roncali, J. *Adv. Funct. Mater.* **2007**, *17*, 1163.
- (20) Roquet, S.; Bettignies, R.; Leriche, P.; Cravino, A.; Roncali, J. *J. Mater. Chem.* **2006**, *16*, 3040.
- (21) Kopidakis, N.; Mitchell, W. J.; Lagemaat, J.; Ginley, D. S.; Rumbles, G.; Shaheen, S.; Rance, W. L. *Appl. Phys. Lett.* **2006**, *89*, 103524.
- (22) Ma, C.-Q.; Fonrodona, M.; Schikora, M. C.; Wienk, M. M.; Janssen, R. A. J.; Baurle, P. *Adv. Funct. Mater.* **2008**, *18*, 3323.
- (23) Jurchescu, O. D.; Baas, J.; Palstra, T. T. M. *Appl. Phys. Lett.* **2004**, *84*, 3061.
- (24) Ostroverkhova, O.; Shcherbyna, S.; Cooke, D. G.; Egerton, R. F.; Hegmann, F. A.; Tykewski, R.; Parkin, S. R.; Anthony, J. E. *J. Appl. Phys.* **2005**, *98*, 033701.
- (25) Sundar, V. C.; Zaumseil, J.; Podzorov, V.; Menard, E.; Willett, R. L.; Someya, T.; Gershenson, M. E.; Rogers, J. A. *Science* **2004**, *303*, 1644.
- (26) Takeya, J.; Yamagishi, M.; Tominari, Y.; Hirahara, R.; Nakazawa, Y.; Nishikawa, T.; Kawase, T.; Shimoda, T.; Ogawa, S. *Appl. Phys. Lett.* **2007**, *90*, 102120.
- (27) Seo, J.-H.; Park, D.-S.; Cho, S.-W.; Kim, C.-Y.; Jang, W.-C.; Whang, C.-N.; Yoo, K.-H.; Chang, G.-S.; Pedersen, T.; Moewes, A.; Chae, K.-H.; Cho, S.-J. *Appl. Phys. Lett.* **2006**, *89*, 163505.
- (28) Lloyd, M. T.; Mayer, A. C.; Subramanian, S.; Mourey, D. A.; Herman, D. J.; Bapat, A. V.; Anthony, J. E.; Malliaras, G. G. *J. Am. Chem. Soc.* **2007**, *129*, 9144.
- (29) Anthony, J. E.; Subramanian, S.; Parkin, S. R.; Park, S. K.; Jackson, T. N. *J. Mater. Chem.* **2009**, *19*, 7984.
- (30) Anthony, J. E.; Purushothaman, B. *SPIE Proc.* **2007**, *6658*, 66580L–8.
- (31) Palilis, L. C.; Lane, P. A.; Kushto, G. P.; Purushothaman, B.; Anthony, J. E.; Kafafi, Z. H. *Org. Electron.* **2008**, *9*, 747.
- (32) Lim, Y.-F.; Shu, Y.; Parkin, S. R.; Anthony, J. E.; Malliaras, G. G. *J. Mater. Chem.* **2009**, *19*, 3049.
- (33) Valentini, L.; Bagnis, D.; Marrocchi, A.; Seri, M.; Taticchi, A.; Kenny, J. M. *Chem. Mater.* **2008**, *20*, 32.
- (34) Marrocchi, A.; Silvestri, F.; Seri, M.; Facchetti, A.; Taticchi, A.; Marks, T. J. *Chem. Commun.* **2009**, 1380.
- (35) Silvestri, F.; Marrocchi, A.; Seri, M.; Kim, C.; Marks, T. J.; Facchetti, A.; Taticchi, A. *J. Am. Chem. Soc.* **2010**, *132*, 6108.
- (36) Schmidtko, J. P.; Friend, R. H.; Kastler, M.; Mullen, K. *J. Chem. Phys.* **2006**, *124*, 174704.
- (37) Wong, W. W. H.; Singh, T. B.; Vak, D.; Pisula, W.; Yan, C.; Feng, X.; Williams, E. L.; Chan, K. L.; Mao, Q.; Jones, D. J.; Ma, C.-Q.; Mullen, K.; Bauerle, P.; Holmes, A. B. *Adv. Funct. Mater.* **2010**, *20*, 927.
- (38) Winzenberg, K. N.; Kemppinen, P.; Fanchini, G.; Bown, M.; Collis, G. E.; Forsyth, C. M.; Hegedus, K.; Singh, T. B.; Watkins, S. E. *Chem. Mater.* **2009**, *21*, 5701.
- (39) Dhanalalan, A.; van Duren, J. K. J.; van Hal, P. A.; van Dongen, J. L. J.; Janssen, R. A. *Adv. Funct. Mater.* **2001**, *11*, 255.
- (40) Meier, H. *Angew. Chem., Int. Ed.* **2005**, *44*, 2482.
- (41) Perzon, E.; Wang, X.; Zhang, F.; Mammo, W.; Delgado, J. L.; Cruz, P.; Inganas, O.; Langa, F.; Andersson, M. R. *Synth. Met.* **2005**, *154*, 53.
- (42) Campos, L. M.; Tontcheva, A.; Günes, S.; Sonmez, G.; Neugebauer, H.; Sariciftci, N. S.; Wudl, F. *Chem. Mater.* **2005**, *17*, 4031.
- (43) Blouin, N.; Michaud, A.; Gendron, D.; Wakim, S.; Blair, E.; Neagu-Plesu, R.; Bellet, M.; Durocher, G.; Tao, Y.; Leclerc, M. *J. Am. Chem. Soc.* **2008**, *130*, 732.
- (44) Roquet, S.; Cravino, A.; Leriche, P.; Alevèque, O.; Frère, P.; Roncali, J. *J. Am. Chem. Soc.* **2006**, *128*, 3459.
- (45) Cravino, A.; Leriche, P.; Alevèque, O.; Roquet, S.; Roncali, J. *Adv. Mater.* **2006**, *18*, 3033.
- (46) Leriche, P.; Frère, P.; Cravino, A.; Alevèque, O.; Roncali, J. *J. Org. Chem.* **2007**, *72*, 8332.
- (47) Zhou, Y.; Peng, P.; Han, L.; Tian, W. *Synth. Met.* **2007**, *157*, 502.
- (48) He, C.; He, Q.; Yang, X.; Wu, G.; Yang, C.; Bai, F.; Shuai, Z.; Wang, L.; Li, Y. *J. Phys. Chem. C* **2007**, *111*, 8661.
- (49) He, C.; He, Q.; Wu, G.; Bai, F.; Li, Y. *SPIE Proc.* **2007**, *6656*, 66560Z.
- (50) He, C.; He, Q.; Yi, Y.; Wu, G.; Bai, F.; Shuai, Z.; Li, Y. *J. Mater. Chem.* **2008**, *18*, 4085.
- (51) Zhao, G.; Wu, G.; He, C.; Bai, F.-Q.; Xi, H.; Zhang, H.-X.; Li, Y. *J. Phys. Chem. C* **2009**, *113*, 2636.
- (52) Zhang, J.; Yang, Y.; He, C.; He, Y.; Zhao, G.; Li, Y. *Macromolecules* **2009**, *42*, 7619.
- (53) Sun, M.; Wang, L.; Du, B.; Xiong, Y.; Liu, R.; Cao, Y. *Synth. Met.* **2008**, *158*, 125.
- (54) Lincker, F.; Delbosc, N.; Bailly, S.; De Bettignies, R.; Billon, M.; Pron, A.; Demadrille, R. *Adv. Funct. Mater.* **2008**, *18*, 3444.
- (55) Xia, P. F.; Feng, X. J.; Lu, J.; Tsang, S.-W.; Movileanu, R.; Tao, Y.; Wong, M. S. *Adv. Mater.* **2008**, *20*, 4810.
- (56) Zhang, W.; Tse, S. C.; Lu, J.; Tao, Y.; Wong, M. S. *J. Mater. Chem.* **2010**, *20*, 2182.
- (57) Xue, L.; He, J.; Gu, X.; Yang, Z.; Xu, B.; Tian, W. *J. Phys. Chem. C* **2009**, *113*, 12911.
- (58) Li, W.; Du, C.; Li, F.; Zhou, Y.; Fahlman, M.; Bo, Z.; Zhang, F. *Chem. Mater.* **2009**, *21*, 5327.
- (59) Yang, Y.; Zhang, J.; Zhou, Y.; Zhao, G.; He, C.; Li, Y.; Andersson, M.; Inganas, O.; Zhang, F. *J. Phys. Chem. C* **2010**, *114*, 3701.
- (60) Shang, H.; Fan, H.; Shi, Q.; Li, S.; Li, Y.; Zhan, X. *Sol. Energy Mater.* **2010**, *94*, 457.
- (61) Liu, Y.; Wan, X.; Yin, B.; Zhou, J.; Long, G.; Yin, S.; Chen, Y. *J. Mater. Chem.* **2010**, *20*, 2464.
- (62) Yin, B.; Yang, L.; Liu, Y.; Chen, Y.; Qi, Q.; Zhang, F.; Yin, S. *Appl. Phys. Lett.* **2010**, *97*, 023303.
- (63) Wallquist, O.; Lenz, R. *Macromol. Symp.* **2002**, *187*, 617.
- (64) Hao, Z.; Iqbal, A. *Chem. Soc. Rev.* **1997**, *26*, 203.
- (65) Wallquist, O. *High-Performance Pigments*, Smith, H. M., Ed.; Wiley-VCH: Weinheim, Germany, 2002; p 159.
- (66) Tamayo, A. B.; Tantiwiwat, M.; Walker, B.; Nguyen, T.-Q. *J. Phys. Chem. C* **2008**, *112*, 15543.
- (67) Tantiwiwat, M.; Tamayo, A. B.; Luu, N.; Dang, X.-D.; Nguyen, T.-Q. *J. Phys. Chem. C* **2008**, 17402.
- (68) Tamayo, A. B.; Walker, B.; Nguyen, T.-Q. *J. Phys. Chem. C* **2008**, *2*, 11545.
- (69) Tamayo, A. B.; Dang, X.-D.; Walker, B.; Seo, J. H.; Kent, T.; Nguyen, T.-Q. *Appl. Phys. Lett.* **2009**, *94*, 103301.
- (70) Peet, J.; Tamayo, A. B.; Dang, X.-D.; Seo, J.-H.; Nguyen, T.-Q. *Appl. Phys. Lett.* **2008**, *93*, 163306.
- (71) To be submitted.
- (72) Tamayo, A.; Kent, T.; Tantiwiwat, M.; Dante, M. A.; Rogers, J.; Nguyen, T.-Q. *Energy Environ. Sci.* **2009**, *2*, 1180.
- (73) Ooi, Z. E.; Tam, T. L.; Shin, R. Y. C.; Chen, Z. K.; Kietzke, T.; Sellinger, A.; Baumgarten, M.; Mullen, K.; deMello, J. C. *J. Mater. Chem.* **2008**, *18*, 4619.
- (74) Shin, R. Y. C.; Sonar, P.; Siew, P. S.; Chen, Z.-K.; Sellinger, A. *J. Org. Chem.* **2009**, *74*, 3293.
- (75) Schubert, M.; Yin, C.; Castellani, M.; Bange, S.; Tam, T. L.; Sellinger, A.; Horhold, H.-H.; Kietzke, T.; Neher, D. *J. Chem. Phys.* **2009**, *130*, 094703.
- (76) Inal, S.; Schubert, M.; Sellinger, A.; Neher, D. *J. Phys. Chem. Lett.* **2010**, *1*, 982.
- (77) Manuscript in preparation.
- (78) Dang, X.-D.; Tamayo, A. B.; Seo, J. H.; Hoven, C.; Walker, B.; Nguyen, T.-Q. *Adv. Funct. Mater.* **2010**, *20*, 3314.
- (79) Sonar, P.; Ng, G.-M.; Lin, T. T.; Dodabalapur, A.; Chen, Z.-K. *J. Mater. Chem.* **2010**, *20*, 3626.
- (80) Karsten, B. P.; Bouwer, R. K. M.; Hummelen, J. C.; Williams, R. M.; Janssen, R. A. *J. Photochem. Photobiol. Sci.* **2010**, *9*, 1055.
- (81) Rousseau, T.; Cravino, A.; Bura, T.; Ulrich, G.; Ziessel, R.; Roncali, J. *Chem. Commun.* **2009**, 1673.
- (82) Rousseau, T.; Cravino, A.; Bura, T.; Ulrich, G.; Ziessel, R.; Roncali, J. *J. Mater. Chem.* **2009**, *19*, 2298.
- (83) Rousseau, T.; Cravino, A.; Ripaud, E.; Leriche, P.; Rihn, S.; De Nicola, A.; Ziessel, R.; Roncali, J. *Chem. Commun.* **2010**, *46*, 5082.
- (84) Kronenberg, N. M.; M. Deppisch, M.; Wurthner, F.; Lademann, H. W. A.; Deing, K.; Meerholz, K. *Chem. Commun.* **2008**, 6489.
- (85) Burckstummer, H.; Kronenberg, N. M.; Gsanger, M.; Stolte, M.; Meerholz, K.; Wurthner, F. *J. Mater. Chem.* **2010**, *20*, 240.
- (86) Silvestri, F.; Irwin, M. D.; Beverina, L.; Facchetti, A.; Pagani, G. A.; Marks, T. J. *J. Am. Chem. Soc.* **2008**, *130*, 17640.
- (87) Bagnis, D.; Beverina, L.; Huang, H.; Silvestri, F.; Yao, Y.; Yan, H.; Pagani, G. A.; Marks, T. J.; Facchetti, A. *J. Am. Chem. Soc.* **2010**, *132*, 4074.
- (88) Mayerhoffer, U.; Deing, K.; Gruss, K.; Braunschweig, H.; Meerholz, K.; Wurthner, F. *Angew. Chem., Int. Ed.* **2009**, 8776.
- (89) Wei, G.; Wang, S.; Renshaw, K.; Thompson, M. E.; Forrest, S. R. *ACS Nano* **2010**, *4*, 1927.
- (90) Mei, J.; Graham, K. R.; Stalder, R.; Reynolds, J. R. *Org. Lett.* **2010**, *12*, 660.
- (91) Varotto, A.; Nam, C.-Y.; Radivojevic, I.; Tome, J. P. C.; Cavaleiro, J. A. S.; Black, C. T.; Drain, C. M. *J. Am. Chem. Soc.* **2010**, *132*, 2552.
- (92) Matsuo, Y.; Sato, Y.; Niinomi, T.; Soga, I.; Tanaka, H.; Nakamura, E. *J. Am. Chem. Soc.* **2009**, *131*, 16048.
- (93) Zhao, X.; Piliego, C.; Kim, B.; Poulsen, D. A.; Ma, B.; Unruh, D. A.; Frechet, J. M. J. *Chem. Mater.* **2010**, *22*, 2325.
- (94) Sharma, G. D.; Suresh, P.; Mikroyannidis, J. A.; Stylianakis, M. M. *J. Mater. Chem.* **2010**, *20*, 561.
- (95) Mikroyannidis, J. A.; Suresh, P.; Sharma, G. D. *Synth. Met.* **2010**, *160*, 932.
- (96) Scharber, M. C.; Muhlbacher, D.; Koppe, M.; Denk, P.; Waldauf, C.; Heeger, A. J.; Brabec, C. J. *Adv. Mater.* **2006**, *18*, 789.